Hydrogen Evolution during Directional Solidification and Its Effect on Porosity Formation in Aluminum Alloys

Q. HAN and S. VISWANATHAN

Most of the models for predicting porosity formation in aluminum alloy castings use a simple mass balance, such as the lever rule, to track hydrogen enrichment in the interdendritic liquid. However, the hydrogen concentration predicted by the lever rule is typically too low to satisfy the threshold concentration for pore nucleation based on classical nucleation and growth theory. As a result, important features of microporosity such as the size and spacing of pores cannot be treated properly. In this article, the hydrogen concentration during the directional solidification of an Al-4.5 pct Cu alloy is calculated, assuming hydrogen rejection during solidification and diffusion in the mushy zone. The calculation shows that the use of the lever rule greatly underestimates the hydrogen concentration at the eutectic front. This is due to the fact that the eutectic front also rejects hydrogen and that this is not considered in the use of the lever rule. Results of numerical simulations that consider hydrogen rejection and diffusion are compared with results obtained using the lever rule. The comparison indicates that actual hydrogen concentrations may be orders of magnitude higher than that predicted by the lever rule. It is suggested that the lever rule should not be used in predicting porosity nucleation. The model outlined in this article is used to propose and explain the formation of a wavelike distribution of pores during directional solidification.

I. INTRODUCTION

POROSITY, which occurs in almost all aluminum alloy castings, is detrimental to the mechanical properties and pressure-tightness of the castings.[1] As a result, research has been conducted on the formation of porosity for almost half a century.[2–9] It is well known that hydrogen is the only gas having a large solubility in the liquid aluminum alloy and a small solubility in the solid. On solidification, hydrogen is rejected by the growing solid and is enriched in the remaining liquid in the mushy zone. When the hydrogen concentration in the liquid exceeds its solubility, pores tend to form. The nucleation and growth of a pore is a process that consumes the supersaturation of hydrogen in the liquid. To model the formation of pores in a casting, both the hydrogen concentration and its solubility in the liquid need to be considered. The partition and diffusion of hydrogen during solidification governs the concentration of hydrogen in the liquid.

Based on the fact that the diffusion coefficient of hydrogen is a few orders of magnitude higher than that of other solute elements in aluminum alloys,[10] the lever rule has been widely employed[4–9] for calculating the local hydrogen concentration in the liquid. The application of the lever rule results in the control volume shown in Figure 1 and a mass balance for hydrogen as shown in Eq. [1]:

$$C_S f_S + C_L f_L = C_0 \qquad [1]$$

where

C_S = the hydrogen concentration in the solid,
C_L = the hydrogen concentration in the liquid,
C_0 = the initial hydrogen concentration of the alloy,
f_S = the local liquid fraction in the mushy zone, and
f_L = the local solid fraction in the mushy zone.

As a result of the use of the lever rule for calculating the local hydrogen concentration, the enrichment of hydrogen in the liquid during solidification is only proportional to the local fraction of solid. This leads to a large error in calculating the hydrogen concentration in the liquid under certain conditions. It is due to the fact that (as will be shown later) hydrogen behaves very differently compared to most other solute elements during solidification. Before pores form, the concentration of hydrogen in the liquid is proportional to the total amount of hydrogen rejected by the solid from the start of solidification. This is shown in the large shaded area shown in Figure 1. For comparison, the control volume representing local f_S and f_L are also shown. As shown in Figure 1, the use of the lever rule using local f_S underestimates the local hydrogen concentration in the liquid. As a result, the calculated hydrogen concentration is typically too low to satisfy the threshold concentration for pore nucleation based on classical nucleation and growth theory. This is one of the reasons why the nucleation and growth of pores cannot be treated properly in numerical models.

This article provides a more complete treatment of hydrogen evolution and diffusion during the solidification of aluminum alloys. In this work, the total hydrogen concentration in the mushy zone of an Al-4.5 pct Cu alloy during directional solidification due to hydrogen diffusion and hydrogen rejection at the advancing solid front is calculated. A comparison is made between the calculated total hydrogen concentration and that predicted using the lever rule. It is hoped that the approach outlined in this article can provide the basis for the development of more sophisticated models that treat the nucleation and the growth of pores during solidification. Although the treatment presented is for directional solidification, the concepts are equally applicable to the case of equiaxed solidification.

Q. HAN, Research Staff Member, and S. VISWANATHAN, Senior Research Staff Member, are with the Oak Ridge National Laboratory, Oak Ridge, TN 37831-6083. Contact e-mail: hanq@ornl.gov
Manuscript submitted October 20, 2000.

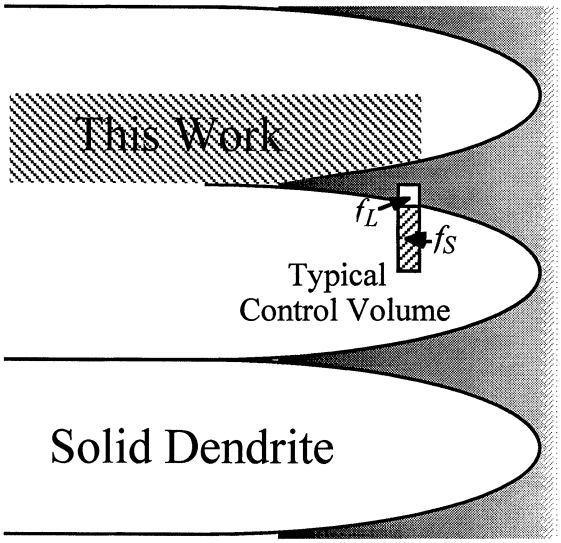

Fig. 1—Schematic diagram showing the control volume element for the application of the lever rule and an improved formulation (large shaded area) that considers the total amount of hydrogen rejected from the start of solidification.

II. HYDROGEN EVOLUTION EQUATIONS

The aluminum-hydrogen phase diagram is shown in Figure 2.[11] In the solid aluminum phase, hydrogen solubility is very small. Ransley and Neufeld showed that the maximum solubility of hydrogen in the solid is about 0.0175 mL/100 g at the melting temperature of pure aluminum metal.[12] Under most casting conditions, the initial hydrogen concentration in the melt is much higher than the maximum solubility of hydrogen in the solid. This means that hydrogen will be rejected to the liquid and enriched in the mushy zone during solidification.

For the calculation of hydrogen evolution during the solidification of an Al-4.5 pct Cu alloy, the solidification is assumed to be one-dimensional and the temperature gradient (G) is assumed to be constant. The total solidification length is assumed to be 30 cm. The growth rate (R) is chosen such that the freezing front is cellular or dendritic, which is the typical morphology of the freezing front during directional solidification. Hydrogen partitioning during solidification is assumed such that the hydrogen concentration in the solid (C_S) is a constant and equal to the maximum solubility of hydrogen in the pure aluminum solid at its melting temperature. The diffusion coefficient of hydrogen in the liquid is taken as 3.8×10^{-3} cm^2/s,[10] and diffusion in the solid is neglected.

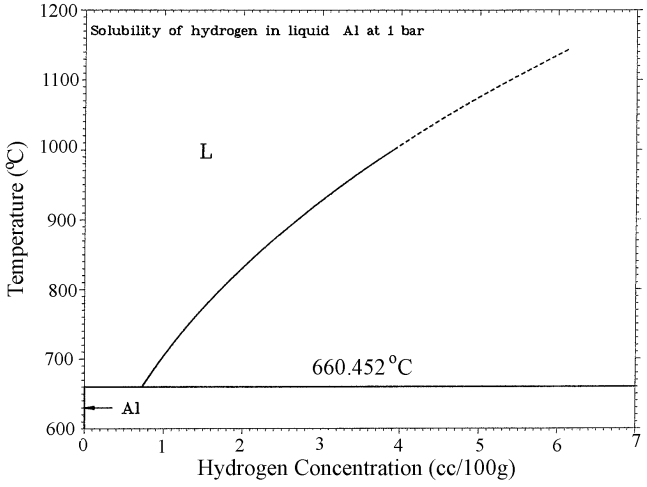

Fig. 2—The aluminum-hydrogen phase diagram.[11]

The evolution of hydrogen is governed by

$$\frac{\partial}{\partial t}(f_L C_L) = \frac{\partial}{\partial x}\left(D f_L \frac{\partial C_L}{\partial x}\right) - C_S \frac{\partial f_L}{\partial t} \qquad [2]$$

where

D = the diffusion coefficient of hydrogen in the liquid,
x = the distance, and
t = the time.

In the all-liquid region where $f_L = 1$ and $\partial f_L/\partial t = 0$, Eq. [2] reduces to a diffusion equation. In the mushy zone, the second term on the right-hand side of Eq. [2] describes the partition of hydrogen between solid and liquid.

Unlike most other solute elements in aluminum alloys, hydrogen does not affect the melting temperature of the solid (Figure 2). Since hydrogen does not affect the melting temperature of the alloy, the liquid fraction (f_L) in the mushy zone is determined only by the copper concentration, so that f_L can be estimated using the Scheil equation.[13,14] Thus,

$$f_L = \left(\frac{T_0 - T}{T_0 - T_L}\right)^{1/(k-1)} \qquad [3]$$

where

T = the temperature in the mushy zone,
T_0 = the melting temperature of pure aluminum,
T_L = the liquidus temperature of the Al-4.5 pct Cu alloy, and
k = the partition coefficient of cooper.

Assuming that x_t is the position of the freezing front (liquidus isotherm), T is given by

$$T = T_L - G(x_t - x) \qquad [4]$$

for a constant temperature gradient of G.

The initial conditions for Eq. [2] are $f_L = 1$, $x_t = 0$, and $C = C_0$. A boundary condition of zero diffusion flux of hydrogen is applied at both ends of the casting (*i.e.*, at $x = 0$ and $x = L$, where L is the length of the casting shown in Figure 3). When the eutectic occurs at the root of the cells/dendrites (*i.e.*, when the eutectic isotherm is at the dendrite roots), hydrogen is rejected at a planar eutectic front at a position x_e. At this position, the usual interface flux balance applies, namely,

$$D \frac{\partial C_L}{\partial x_e} = R(C_L - C_S) f_E \qquad [5]$$

where f_E is the eutectic fraction. Using these initial and boundary conditions, Eq. [2] can be solved numerically to calculate *the total hydrogen concentration* in the liquid as a function of distance.

III. RESULTS AND DISCUSSION

For purposes of illustration, hydrogen evolution during the directional solidification of an Al-4.5 pct Cu alloy with an

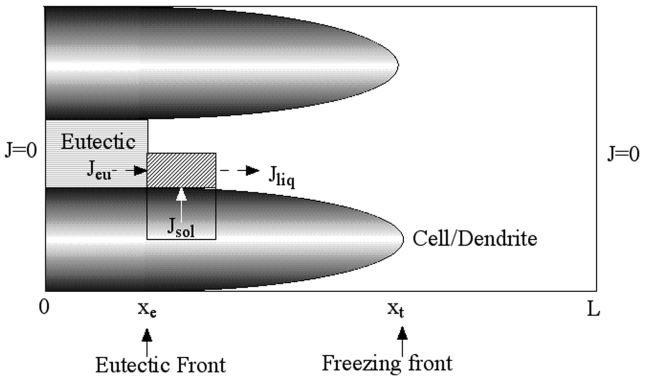

Fig. 3—Schematic illustration showing the various fluxes that must be taken into account in calculating hydrogen redistribution during directional solidification, *viz.*, hydrogen partitioning during primary solidification, hydrogen diffusion toward and beyond the dendrite tips, and hydrogen rejection at the eutectic front.

initial hydrogen concentration of 0.1 mL/100 g is considered. The solidification conditions are assumed to be $R = 10^{-2}$ cm/s and $G = 1$ °C/cm. The hydrogen concentration in the liquid and the corresponding liquid fraction in the mushy zone are plotted against distance for the solidification length of 30 cm.

Hydrogen evolution during solidification is best understood by analyzing hydrogen evolution in two stages. In the first stage, the liquid fraction at $x = 0$ is greater than the eutectic fraction of 0.081, *i.e.*, the temperature at $x = 0$ is greater than the eutectic temperature. This is illustrated in Figure 4. Until the onset of the eutectic, hydrogen is progressively enriched in the liquid due to the difference in solubility between the solid and the liquid. Hydrogen also diffuses toward and ahead of the dendrite tips. The upper plot in Figure 4 shows the hydrogen concentration as a function of distance, while the lower plot shows the corresponding liquid fraction. In the upper plot in Figure 4, both the hydrogen concentration calculated using the lever rule (Eq. [1]) and calculated total hydrogen concentration are plotted for comparison. When the liquid fraction is higher than the eutectic fraction, the calculated total hydrogen concentration is actually slightly lower than that for the lever rule, due to hydrogen diffusing toward and beyond the dendrite tips.

This scenario changes dramatically in the second stage of hydrogen evolution, when the eutectic appears. Due to the large difference in solubility between the solid and the liquid, a significant amount of hydrogen is rejected at the eutectic front when the highly enriched eutectic liquid solidifies. Provided that pore nucleation does not occur, the hydrogen concentration at the eutectic front increases drastically as the eutectic front advances. As shown in Figure 5, the hydrogen concentration is 8 mL/100 g when the eutectic front advances a distance of 3.15 cm ($x_e = 3.15$ cm), *i.e.*, about 80 times its original concentration, and is 20 mL/100 g when $x_e = 9.15$ cm, about 200 times its original concentration. Although the hydrogen concentration decreases rapidly away from the eutectic front, the highly enriched zone of hydrogen still extends a few centimeters ahead of the eutectic front. The dashed curve at the top of Figure 5 indicates the locus of the maximum hydrogen concentration at the eutectic front as a function of position, in the absence of pore nucleation.

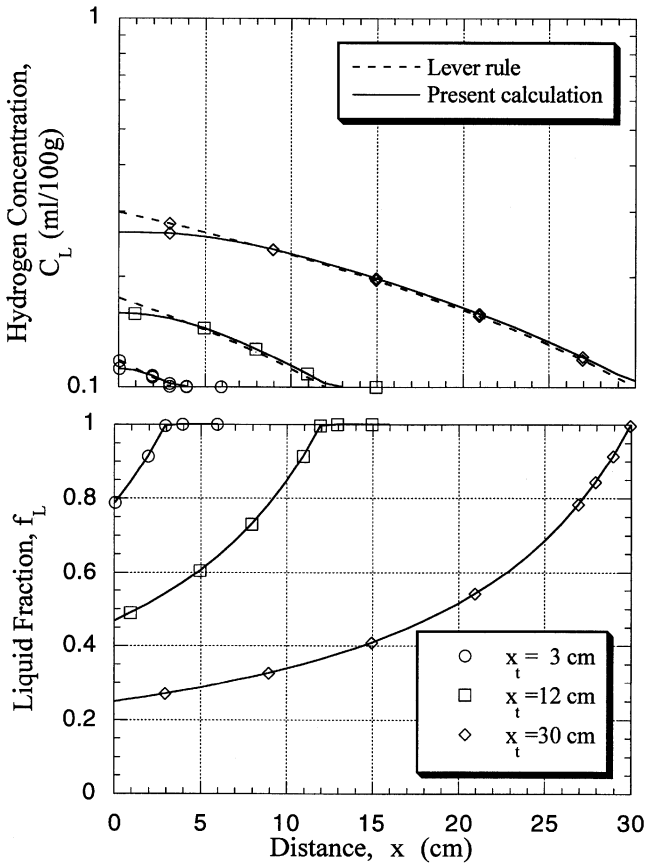

Fig. 4—Evolution of hydrogen during the first stage of directional solidification of an A1-4.5 pct Cu alloy containing 0.1 mL/100 g hydrogen when the liquid fraction at $x = 0$ is higher than the eutectic fraction of 0.081. The top diagram shows both the hydrogen concentration in the liquid calculated using the lever rule and that from the present calculation. The bottom diagram shows the corresponding liquid fraction.

Keeping in mind that the liquid fraction at the eutectic front is always equal to f_E (*i.e.*, 0.081), the use of the lever rule would predict a fixed hydrogen concentration at the eutectic front, given by the mass balance shown in Eq. [1]. This results in a hydrogen enrichment of only about 10 times the initial concentration. This is obviously much smaller than the values obtained with the present calculation and is unlikely to result in pore nucleation based on classical nucleation and growth theory.

The previous calculations point out an important aspect of the calculation of the redistribution of solute elements such as hydrogen, which are rejected at the eutectic front. The lever rule and the Scheil equation cannot be used to predict the hydrogen concentration in the interdendritic liquid, as hydrogen is rejected at the eutectic front. As shown in Figure 3, the hydrogen partitioning during solidification, the hydrogen diffusing toward and beyond the dendrite tips, and the hydrogen rejected at the eutectic front must be considered. Care should also be taken in the use of the lever rule or the Scheil Equation for calculating solute redistribution in multicomponent alloys, as there should be long-distance diffusion of some solute elements and rejection of some solute elements at the eutectic front.

Figures 6 through 8 show the calculated maximum hydrogen concentration at the eutectic front for varying temperature gradients, initial hydrogen concentrations, and growth

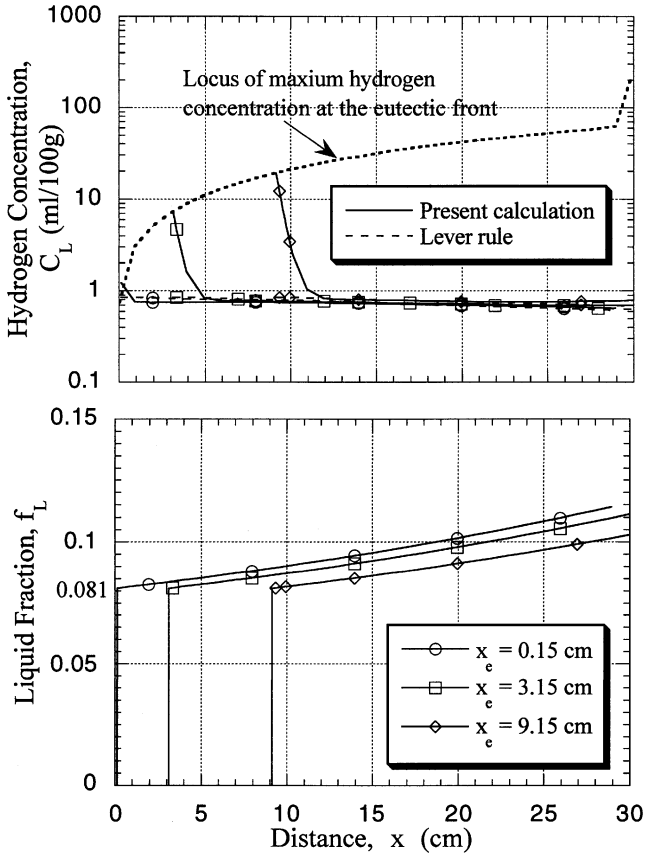

Fig. 5—Evolution of hydrogen during the second stage of directional solidification of an Al-4.5 pct Cu alloy containing 0.1 mL/100 g hydrogen when the eutectic reaction occurs. The top diagram shows both the hydrogen concentration in the liquid calculated using the lever rule and that from the present calculation. The locus of the maximum hydrogen concentration at the eutectic front is also shown. The bottom diagram shows the corresponding liquid fraction.

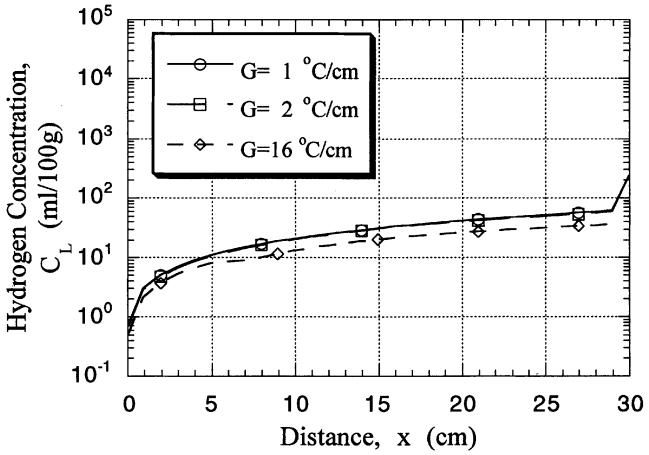

Fig. 6—Calculated total hydrogen concentration at the eutectic front for C_0 = 0.1 mL/100 g, R = 0.01 cm/s, and thermal gradients of 1, 2, and 16 °C/cm. Pore nucleation is neglected.

rates of the solid. An increase in the temperature gradient decreases the hydrogen concentration at the eutectic front (Figure 6), due to greater hydrogen diffusion toward the dendrite tip, but the decrease is very small. Even with a

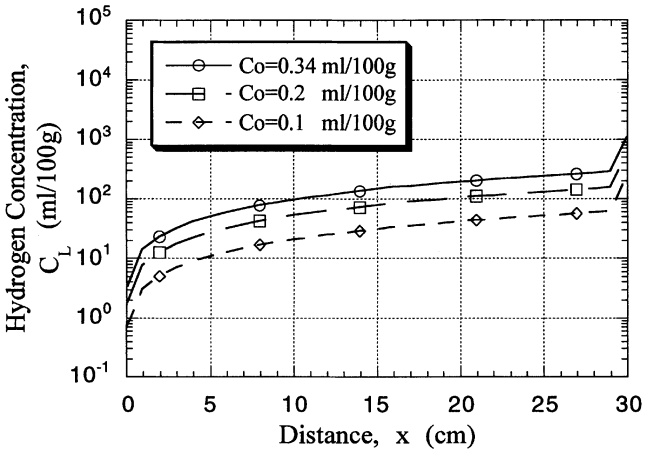

Fig. 7—Calculated total hydrogen concentration at the eutectic front for G = 1.0 °C/cm, R = 0.01 cm/s, and initial hydrogen levels of 0.1, 0.2, and 0.34 mL/100 g. Pore nucleation is neglected.

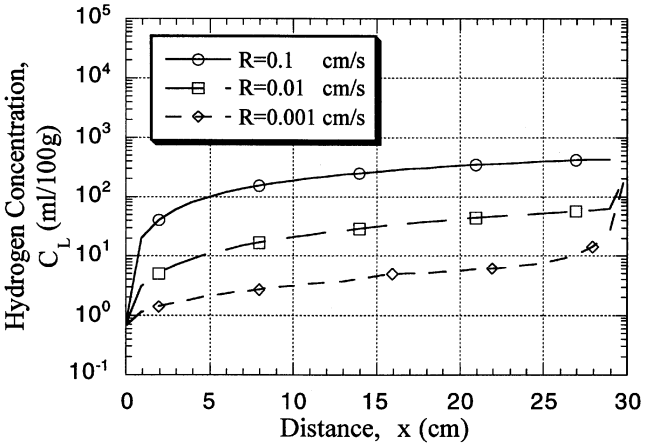

Fig. 8—Calculated total hydrogen concentration at the eutectic front for C_0 = 0.1 mL/100 g, G = 1.0 °C/cm, and growth rates of 0.001, 0.01, and 0.1 cm/s. Pore nucleation is neglected.

temperature gradient of 16 °C/cm, the hydrogen concentration at the eutectic front is much higher than that predicted using the lever rule.

The initial hydrogen concentration affects the hydrogen concentration at the eutectic front (Figure 7). An increase in the initial hydrogen concentration results in a proportional increase in the hydrogen concentration at the eutectic front.

The most important parameter affecting the hydrogen concentration at the eutectic front is the growth rate of the solid, assuming that the solubility of hydrogen in the solid is not affected by the growth rate. As shown in Figure 8, the calculated hydrogen concentration at the eutectic front increases drastically with increasing growth rate of the solid. This indicates that the nucleation of porosity is likely to be favored at high growth rates of solid. However, the porosity level may not necessarily be higher, since the increased nucleation is only likely to result in a larger number of small pores. In the example considered in this study, the higher growth rates of the solid correspond to larger cooling rates, since the cooling rate is the product of the thermal gradient and growth rate. In this case, the pore size will most likely decrease, since the secondary dendrite arm spacing decreases

with increasing cooling rate.[15] Similarly, the pore fraction would also likely decrease at increasing cooling rates.[6]

The enrichment of hydrogen at the eutectic front leads to the postulation of a wavelike distribution of pores during directional solidification. As illustrated in Figure 9, hydrogen becomes enriched at the cell/dendrite root as the freezing front advances. When the hydrogen concentration reaches a critical value (C_C), pore nucleation occurs. The nucleation and the subsequent growth of the pore consumes hydrogen locally and reduces the local hydrogen concentration in the liquid to a level corresponding to that of equilibrium between the hydrogen in the pore and that in the liquid. The growth of the pores ceases, and the pores will most likely be gradually trapped by the growing solid. As the freezing front advances further, hydrogen will again be enriched in the liquid until pore nucleation occurs. As a result, pores will occur periodically in a wavelike fashion (Figure 9). This was observed by Carte[16] during the rapid freezing of a thin layer of water. In the case of the freezing of water, the dissolved gas is air. The wavelike distribution of gas bubbles in ice is directly related to hydrogen evolution and the subsequent nucleation and growth of pores in aluminum alloys. If this distribution can be documented experimentally, the critical supersaturation required for hydrogen bubble nucleation can be estimated by measuring the distance corresponding to the location of the first pore in a directionally solidified sample.

Under most casting conditions, pores are not distributed in a wavelike fashion; instead, they are distributed more or less uniformly in the casting. This is due to the fact that pores migrate toward the direction of the higher liquid fraction in the mushy zone. The pore migration blurs the wavelike distribution of porosity in a casting. In the solidification of cyclohexane, a transparent alloy, it was observed that pores could migrate over a large distance and that their migration velocities could be as high as 200 μm/s.[17] Unfortunately, this suggests that important aspects of porosity formation, such as the critical hydrogen supersaturation required for nucleation and information on hydrogen diffusion, cannot be easily obtained from the distance between pores in a casting. Pore migration during solidification needs to be systematically studied and quantified in order to fully understand the final distribution of pores in a casting.

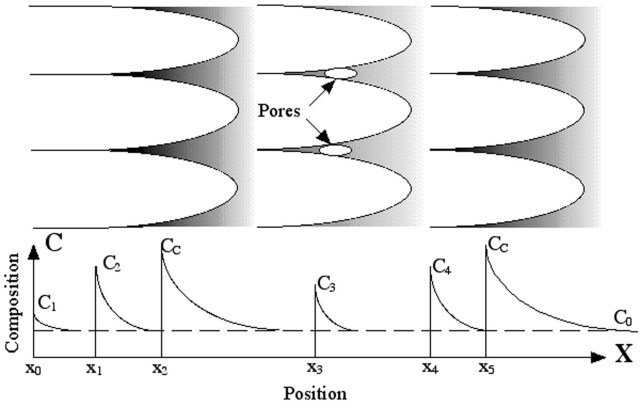

Fig. 9—Schematic illustration showing the formation of a wavelike distribution of pores during directional solidification. Here, x_0 through x_5 denote the positions of the eutectic isotherm, and C denotes the hydrogen concentration in the liquid ahead of the eutectic isotherm.

IV. CONCLUSIONS

The use of the lever rule for the prediction of the hydrogen concentration in the liquid in the mushy zone underestimates the hydrogen concentration at the eutectic front during the solidification of aluminum alloys. Models for predicting pore nucleation, size, and distribution should not use the lever rule for calculating hydrogen concentration, since the predicted hydrogen concentrations are too low to satisfy the threshold concentration for pore nucleation based on classical nucleation and growth theory. Calculations of the total hydrogen concentration at the eutectic front that consider hydrogen partitioning during primary solidification, hydrogen diffusion toward the dendrite tips, and hydrogen rejection at the eutectic front indicate that actual hydrogen concentrations may be orders of magnitude higher than that predicted by the lever rule.

The enrichment of hydrogen at the eutectic front is strongly affected by the growth velocity of the solid, with higher growth rates leading to significantly higher enrichment of hydrogen at the eutectic front. Hydrogen enrichment at the eutectic front also increases with an increase in the initial hydrogen concentration in the liquid. However, the hydrogen concentration at the eutectic front is only slightly dependent on the thermal gradient. An increase in the thermal gradient leads to a somewhat lower hydrogen concentration at the eutectic front.

The enrichment of hydrogen at the eutectic front leads to the postulation of a wavelike distribution of pores after solidification. However, under most solidification conditions, this wavelike distribution of pores is likely blurred by pore migration in the mushy zone.

ACKNOWLEDGMENTS

This work was performed under a Cooperative Research and Development Agreement (CRADA) with the United States Advanced Materials Partnership (USAMP), United States Council for Automotive Research (USCAR), for the project on Design and Product Optimization for Cast Light Metals. The research was sponsored by the United States Department of Energy, Assistant Secretary for Energy Efficiency and Renewable Energy, Office of Transportation Technologies, Lightweight Vehicle Materials Program, under Contract No. DE-AC05-00OR22725 with UT–Battelle, LLC. The authors thank S.S. Babu and A.S. Sabau for reviewing the article and M.L. Atchley for preparing the manuscript.

REFERENCES

1. J. Campbell: *Castings*, Butterworth-Heinemann, Oxford, United Kingdom, 1991, p. 282.
2. W.D. Walther, C.M. Adams, and H.F. Taylor: *Trans. AFS*, 1956, vol. 64, pp. 658-64.
3. T.S. Piwonka and M.C. Flemings: *Trans. TMS-AIME*, 1966, vol. 236, pp. 1157-65.
4. K. Kubo and R.D. Pehkle: *Metall. Trans.*, 1985, vol. 16B, pp. 359-66.
5. D.R. Poirier, K. Yeum, and A.L. Maples: *Metall. Trans.*, 1987, vol. 18A, pp. 1979-87.
6. Q.T. Fang and D.A. Granger: *Trans. AFS*, 1989, vol. 97, pp. 989-1000.
7. S. Shivkumar, D. Apelian, and J. Zou: *Trans. AFS*, 1990, vol. 98, pp. 897-907.

8. P.D. Lee: Ph.D. Thesis, University of Oxford, Oxford, United Kingdom, 1994.
9. A.S. Sabau and S. Viswanathan: *Light Metals 2000*, R.D. Peterson, ed., TMS-AIME, Warrendale, PA, 2000, pp. 597-602.
10. W. Eichenauer and J.Z. Markopoulos: *Z. Metallkd.*, 1974, vol. 65, pp. 649-52.
11. *Binary Phase Diagrams*, T.B. Massalski, ed., ASM, Metals Park, OH, 1986.
12. C.E. Ransley and H. Neufeld: *J. Inst. Met.*, 1948, vol. 74, pp. 599-20.
13. W. Kurz and D.J. Fisher: *Fundamentals of Solidification*, 3rd ed., Trans Tech Publications, Aerdermannsdorf, Switzerland, 1989, p. 158.
14. T.F. Bower, H.D. Brody, and M.C. Flemings: *Trans. AIME*, 1966, vol. 236, pp. 624-34.
15. Q. Han, H. Hu, and X. Zhong: *Metall. Mater. Trans.*, 1997, vol. 28B, pp. 1185-87.
16. A.E. Carte: *Proc. Phys. Soc.*, 1961, vol. 77, pp. 757-68.
17. Q. Han and S. Viswanathan: Oak Ridge National Laboratory, Oak Ridge, TN, unpublished research, 1999.